



BIOMETRIC PERSONAL IDENTIFICATION ON 2D WAVELET TRANSFORM AND CHI-SQUARED MODEL

TaiwoTundeAdeniyi<adetokis@gmail.com>
Olatubosun Olabode<oolabode@futa.edu.ng>
Gabriel B. Iwasokun<gbiwasokun@futa.edu.ng>
, Samuel A. Oluwadare<saoluwadare@futa.edu.ng>
Raphael O.Akinyede<roakinyede@futa.edu.ng>
Computer Science Department
Federal University of Technology, Akure

ABSTRACT

Iris recognition system consists of image acquisition, iris preprocessing, iris segmentation and feature extraction with comparison (matching) stages. The biometric based personal identification using iris requires accurate iris segmentation for successful identification or recognition. Recently, several researchers have implemented various methods for segmentation of boundaries which will require a modification of some of the existing segmentation algorithms for their proper recognition. Therefore, this research presents a 2D Wavelet Transform and Chi-squared model for iris features extraction and recognition. Circular Hough Transform was used for the segmentation of the iris image. The system localizes the circular iris and pupil region and removes the occluding eyelids and eyelashes. The extracted iris region is normalized using Daugman's rubber sheet model into a rectangular block with constant dimensions to account for imaging inconsistencies. Finally, the phase data (iris signature) from the 2D wavelet transform data is extracted, forming the biometric template. The chi-squared distance is employed for classification of iris templates and recognition. Implementing this model can enhance identification. Based on the designed system, an FAR (False Acceptances ratio) of 0.00 and an FRR (False Rejection Ratio) of 0.896 was achieved.

Keyword

Daugman, Iris, 2DWave length, Chi-square, Identification

Council for Innovative Research

Peer Review Research Publishing System

Journal: INTERNATIONAL JOURNAL OF COMPUTERS & TECHNOLOGY

Vol.14, No. 9

www.ijctonline.com, editorijctonline@gmail.com



1.0 INTRODUCTION

Biometric authentication has been receiving extensive attention over the last decade, with increasing demands in automated personal identification (Quinchun and Shukur, 2013). Biometrics is an automated method of identifying a person or verifying the identity of a person based on physiological or behavioral characteristics. Examples of physiological characteristics include finger print and iris recognition. Behavioral characteristics are learned or acquired. Examples of behavioral characteristics are signature verification, walking pattern and speaker verification. Physiological characteristics are unique to individuals and cannot be copied and hence responsible for their reliability and accuracy (Sunita and Vishram, 2012).

Iris recognition is regarded as the most reliable and accurate biometric identification system available because the probability of finding two identical iris patterns is considered to be approximately 1 in 1052 (Mohd, 2013). As an important and distinct characteristic for status, the iris has many advantages such as uniqueness, stability, and so on (Sunita, 2012; Kekre, 2010). Comparing with the fingerprint, the face and other status identification methods, the iris has the higher accuracy (Sunita, 2012). The human iris lies in between the white sclera and the pupil which appear black in image. The iris begins to form in the third month of gestation and the structures creating its pattern are largely complete by the eight months, although pigment accretion can continue in the first postnatal years. Its complex pattern can contain many distinctive features such as arching ligaments, furrows, ridges, crypts, rings corona, freckles and zigzag collaret (Daugman, 2004). These visible characteristics, which are generally called the texture of the iris, are unique to each subject.

The state-of-the-art iris recognition was presented in Daugman, (2007) using Gabor wavelets. That system has since been widely implemented and tested. Recently, other researchers including the work of (Wildes, 1997; 2011) on iris segmentation using integro differential operator, (Boles and Boashash, 1998) on iris recognition algorithm based on zero-crossing detection of the wavelet transform and on Phase correlation method. Several methods for iris recognition have been proposed (Tan, 2005), however most of them focused on using statistical features such as mean and variance as feature vectors. Liam et.al., (2004) tried to extract more distinctive statistical features by using filtering process. However, some critical problems still persist and significant work needs to be done before mass-scale deployment. Many issues, including system robustness, speed of enrollment and accuracy of recognition remain to be addressed.

The iris color is not employed in iris recognition because it has a limitation that people with the same genotype have a higher chance of having similar color content in their iris region. However, the textural pattern is unique and hence the use in iris recognition. Iris recognition systems are divided into four blocks; preprocessing, iris segmentation, iris normalization, and feature extraction. Iris preprocessing prepares the captured eye image for segmentation (converting image to grayscale, noise removal, etc.). Iris segmentation separates the iris region from the entire captured eye image. Iris normalization fixes the dimensions of segmented iris region to allow for accurate comparisons. Feature extraction draws out the biometric templates from the normalized image to form the iris signature or the feature vector and matches this template with reference templates. The matching is done using the chi-squared model. The performance of an iris system closely depends on the precision of the iris segmentation (Matsoso, 2013).

In this Research work, a different approach of using the distance measure between two iris images is considered. A chi-square and 2D wavelet transform are used as feature sets which are transformed into a distance domain using a distance computation which are stored in the database for matching or comparison purpose. To test the proposed system a database of iris developed by the Chinese Academy of Sciences Institute of Automation (CASIA) is used. To evaluate the performance of the proposed iris recognition system, two important factors; the False Acceptance Rate (FAR) and the False Rejection Rate (FRR) of genuine iris images submitted is estimated.

2.0 Literature Review

In Monaheng and Kuruba, (2013), a system was proposed that uses circular Hough transform to deduce the radius and centre coordinates of the pupil and iris regions. Hough transform was used for detection of circles and other parameterizable geometric figures. The results of the study provided 95.6 % accuracy. The limitation is that in most cases where the boundary of the iris is covered by the eyelids circular Hough transform is not enough to get rid of the eye lids and hence a linear Hough transform is needed and reflection on the iris images needs to be correct for an even comparison. Combining two models to detect the iris region increases the time taken to enroll an iris image.

The paper Kekre, Thepade, Jain and Agrawal, (2010) on the use of Haar Wavelets at various levels of decomposition for feature extraction provided an information that Haarlets level-5 outperforms other Haarlets, because the higher level Haarlets gave very fine texture features while the lower level Haarlets represents very coarse texture features which are less useful for discrimination of images in iris recognition. However generating up to 5 level of the Haarlet is time consuming and affects the overall efficiency of the system. The paper of Jin, Tong, Pengge and Shukui, (2013) presents a novel iris recognition based on windowed gray difference histogram of sub-regions (Choi et.al., 2010). The key points are detected by scale-space extrema of difference-of-Gaussian function from the normalized iris images. The system was tested on CASIA database and had a correct recognition rate of 96.69% and equal error rate of 0.42. The robustness of the system could be improved and also there was no room for noise removal in the system.

The objective of Mabrukar, Sonawane and Bagban, (2013), was to show that feature extraction using Multi-scale Taylor expansion also yields good results and using Multi-scale Taylor series Expansion helps in reducing the size of the iris template which is vital for efficient processing in large-scale application. The method uses phase based features from the multi-scale Taylor expansion. Using Phase-based iris recognition algorithms improves speed of operation and also



increases verification performance (Daugman, 2007). The iris recognition system employed, extracts features from binarized multi-scale Taylor expansion phase information. For the binary feature vector, code "0" corresponds to a negative sign of the expansion and similarly, code "1" corresponds to positive sign of the expansion. However, performing multi-scale Tailors-series does not fully exploit the available features in the segmented iris image.

In the paper of Lokhande and Bapat, (2012), a novel multi-resolution approach based on Wavelet Packet Transform (WPT) was proposed for iris texture analysis and recognition. The development of this approach is motivated by the observation that dominant frequencies of iris texture are located in the low and middle frequency channels. The experiment provided a 93% correct classifications when the algorithm is applied on an iris image database. The assumption is that the input image is a clear image and hence no filtering model employed. The paper Kaur, Girdhar and Kaur, (2010) discusses the enhanced iris recognition which is used to overcome some of the problem such as to automate the recognition of the iris by reducing complexity and increasing algorithm speed. Canny Edge Detection was used to generate an edge map of the iris image as part of the pre-processing method and in order to increase the overall speed of the system and a circle detection algorithm was used for segmentation. The paper presents an automated and novel iris recognition system where overall computational match speed is reduced and hence makes system more reliable with accuracy of 99.38% and low FAR. Image segmentation techniques or noise removal methods can be improved, so that the input image to the feature extraction stage could be made better which can improve the final outcome. Also, the validity of the system's robustness needs to be verified.

This article Rydgren, Ea, Amiel, Rossant and Amara, (2004) presents an application of wavelet packet analysis to the features extraction part of an iris recognition system. An energy measure is used to identify the particular packet that carries discriminating information about the iris texture. The geometry of the iris is circular and most of its interesting textural features are extended in the radial and to a lower extent the angular direction. Therefore, analysis is simplified by an adapted polar transform, suggested by Daugman (Daugman, 1993). The normalization was done using the Daugman's rubber model. Packets gave a good description of the frequency content of an image. The sub-images in the wavelet packet tree holds information about both frequency (scale) and localization as opposed to, for example, the Fourier transform that only hold frequency information. However, the performance of Gabor wavelet is so far superior but it is likely that the performance of the wavelet packets algorithm can be increased in the future.

The paper Daugman, (2004) explains the iris recognition algorithms. The integro-differential operator was used for the localization of the iris image. The mathematical model is stated below;

$$\text{Max}_{(r,x_0,y_0)} |G_\sigma(r) * \frac{\partial}{\partial r} \oint_{r,x_0,y_0} \frac{I(x,y)}{2\pi r} ds|$$

where $I(x; y)$ is an image. The operator searches over the image domain $(x; y)$ for the maximum in the blurred partial derivative with respect to increasing radius r , of the normalized contour integral of $I(x; y)$ along a circular arc ds of radius r and center coordinates $(x_0; y_0)$. The symbol $*$ denotes convolution and $G_\sigma(r)$ is a smoothing function such as a Gaussian of scale σ .

In Patil and Patil, (2009) a wavelet-based quality measure for iris images was proposed. The proposed method includes three modules: image preprocessing, feature extraction and recognition modules. The feature extraction module adopts the wavelet transform as the discriminating features. Similarity between two iris images is estimated using Euclidean distance measures. Features extracted using higher level wavelet decompositions are shown to yield better clustering and higher success rate in recognition. The Euclidean distance was used as a way of defining the closeness of match between two iris feature templates. It is calculated by measuring the norm between two vectors.

$$D = \text{sqrt}\{(x_2 - x_1)^2 + (y_2 - y_1)^2\}$$

The Proposed model in Gulmire and Ganorkar, (2012) for features extraction was ICA (Independent Component Analysis). For segmentation purpose Daugman method is used. Images of eyes from 10 persons were used, and every person has six images of eyes. The top three images are used as test images and the next three images are used for training purpose. Daugman's method was used for iris regions segmentation and Independent Component Analysis used for feature extraction. In the identification stage the Euclidean distance between a test image and a training image was calculated. The smallest distance among them shows whether the test image belongs to this class. The recognition rate is 89.5%.

3.0 Proposed System Design

3.1 Iris Image Preprocessing

First of all, the input image from webcam or captured image is needed for further preprocessing. Special cameras are available for capturing the iris. The captured image or saved image is a .jpg file (joint pictures group). How well the captured or saved image appears depend on the quality of the capturing device. The resolution of the iris capturing device determines the quality of the images (iris images captured). There are several cameras available for this purpose, however there are high tendencies of noise being introduced. Noise is unwanted parts of an image introduced during the acquisition of the image (Robert, 2010; Mythili, 2011; Pierre, 2004). For any biometric system, image acquisition is the first step to recognition. Iris images can be captured by the use of electronic devices or be downloaded from online (Bakstein, 2013). In this study, iris images were obtained from online (CASIA database and UbiS database).



After getting the iris image, the iris image went through the preprocessing stage. The preprocessing stage involves the conversion of the image to greyscale and then detecting the edges using the canny edge algorithm. The output of the preprocessing stage is a binary image showing the edges in the iris image. The next stage is the segmentation stage which involves detecting the iris and pupil boundary. The segmentation was done using the Circular Hough transform. Usually two circles are drawn to indicate the iris and pupil boundary. The next stage is the normalization stage which is meant to remove the effect of illumination, light intensity, head tilt from the segmented iris image. The Daugman's rubber sheet model was used for the normalization of the image into a fixed dimension. Features extraction followed the normalization stage which involves the generation of the feature vectors. A 2D wavelet transform was used for the feature extraction. After the feature extraction, the distance was computed.

3.2 Greyscale Conversion

The captured image or downloaded image is converted to a grayscale image as this is necessary for the canning edge algorithm. For a black-and-white image, a light with $c(\lambda)$ can be represented by one number I given by

$$I = k \int_{\lambda=0}^{\infty} c(\lambda) s_{BW}(\lambda) d\lambda \tag{1}$$

where $s_{BW}(\lambda)$ is the spectral characteristic of the sensor used and k is some scaling constant. The value I is often referred to as the luminance, intensity, or gray level of a black-and-white image represents power per unit area, it is always non-negative and finite, that is,

$$0 \leq I \leq I_{MAX}$$

where I_{MAX} is the maximum I possible. In image processing, I is typically scaled such that it lies in some convenient arbitrary range, for example, $0 \leq I \leq 255$. In these cases 0 corresponds to the darkest possible level and 1 or 255 corresponds to the brightest possible level. Because of this scaling, the specific radiometric or photometric units associated with I become unimportant. A black-and-white image has, in a sense, only one color. Thus, it is sometimes called a monochrome image.

A color image can be viewed as three monochrome images. For a color image, a light with $c(\lambda)$ is represented by three numbers which are called *tristimulus values*. One three-number set that is frequently used in practice is R, G, and B, representing the intensity of the red, green, and blue components. The tristimulus values R, G, and B are obtained by

$$R = k \int_{\lambda=0}^{\infty} c(\lambda) s_R(\lambda) d\lambda ; \quad G = k \int_{\lambda=0}^{\infty} c(\lambda) s_G(\lambda) d\lambda \quad ; \quad B = k \int_{\lambda=0}^{\infty} c(\lambda) s_B(\lambda) d\lambda$$

where $s_R(\lambda)$, $s_G(\lambda)$, and $s_B(\lambda)$ are spectral characteristics of the red, green, and blue sensors (filters) respectively. Like the gray level I in a monochrome image, R, G, and B are non-negative and finite. .

3.3 Edge Detection

Detection of object boundaries is an important part of perception process (Poonam and Neha, 2013; Patil, 2009; Bo, 2013). Edge detection techniques aims to find local discontinuities in some image attribute such as intensity or color. These discontinuities are of interest because they are likely to occur at the boundaries of objects, but local edges may also occur due to variations in surface characteristics of an object, changes in illumination and shadows and the like.

A crucial step in this method is to capture the intuitive criteria given (good detection, good localization and only one response to a single edge) in a mathematical form which is readily solvable. First with signal-to-noise ratio and localization. Let the impulse response of the filter be $f(x)$ and denote the edge itself by $G(x)$. Assume that the edge is centered at $x = 0$. Then the response of the filter to this edge at its center H_G is given by a convolution integral (considering a one dimensional profile) (Canny, 1986):

$$H_G = \int_{-W}^{+W} G(-x)f(x)dx \tag{2}$$

Assuming the filter has a finite impulse response bounded by $[-W, W]$. The root-mean-squared response to the noise $n(x)$ only, will be

$$H_n = n_0 \left[\int_{-W}^{+W} G(-x)f(x)dx \right]^{1/2} \tag{3}$$

Where n_0^2 is the mean-squared noise amplitude per unit of length. The first criterion, the output signal-to-noise ratio (SNR), is the quotient of these two responses.

$$SNR = \frac{\left| \int_{-W}^{+W} G(-x)f(x)dx \right|}{n_0 \sqrt{\int_{-W}^{+W} f^2(x)dx}} \tag{4}$$



For the localization criterion, Canny wants some measure which increases as localization improves, and will use the reciprocal of the root-mean-squared distance of the marked edge from the center of the true edge. Marking edges at local maxima in the response of the operator $f(x)$, the first derivative of the response will be zero at these points. Note also that since edges are centered at $x = 0$, in the absence of noise there should be a local maximum in the response at $x = 0$. Let $H_n(x)$ be the response of the filter to noise only, and $H_G(x)$ be its response to the edge, and suppose there is a local maximum in the total response at the point $x = x_0$. Then

$$H'_n(x_0) + H'_G(x_0) = 0 \tag{5}$$

The Taylor expansion of $H'_G(x_0)$ about the origin gives

$$H'_G(x_0) = H'_G(0) + H''_G(0)x_0 + O(x_0^2) \tag{6}$$

By assumption $H'_G(0) = 0$, i.e., the response of the filter in the absence of noise has a local maximum at the origin, so the first term in the expansion can be ignored. Equations (5) give

$$H''_G(0)x_0 \approx -H'_n(x_0) \tag{7}$$

Now $H'_n(x_0)$ is a Gaussian random quantity whose variance is the mean-squared value of $H'_n(x_0)$, and is given by

$$E[H'_n(x_0)^2] = n_0^2 \int_{-w}^{+w} f'^2 dx \tag{8}$$

where $E[y]$ is the expectation value of y . Combining this result with (7) and substituting for $H''_G(0)$ gives

$$E[x_0^2] \approx \frac{n_0^2 \int_{-w}^{+w} f'^2 dx}{[\int_{-w}^{+w} G'(-x)f'(x) dx]^2} = \delta x_0^2 \tag{9}$$

where δx_0 is an approximation to the standard deviation of x_0 . The localization is defined as the reciprocal of δx_0 .

$$Localization = \frac{|\int_{-w}^{+w} G'(-x)f'(x) dx|}{n_0 \sqrt{\int_{-w}^{+w} f'^2(x) dx}} \tag{10}$$

Equations (4) and (10) are mathematical forms for the first two criteria, and the design problem reduces to the maximization of both of these simultaneously. In order to do this, it is important to maximize the product of (4) and (10). One could conceivably have combined (4) and (10) using any function that is monotonic in two arguments, but the use of the product simplifies the analysis for step edges. For the present let us make use of the product of the criteria for arbitrary edges, i.e., seeking to maximize

$$\frac{|\int_{-w}^{+w} G(-x)f(x) dx|}{n_0 \sqrt{\int_{-w}^{+w} f^2(x) dx}} \frac{|\int_{-w}^{+w} G'(-x)f'(x) dx|}{n_0 \sqrt{\int_{-w}^{+w} f'^2(x) dx}} \tag{11}$$

There may be some additional constraints on the solution, such as the multiple response constraint described next.

3.4 Eliminating Multiple Responses

In the specification of the edge detection problem, Canny decided that edges would be marked at local maxima in the response of a linear filter applied to the image. The detection criterion given above measured the effectiveness of the filter in discriminating between signal and noise at the center of an edge. It does not take into account the behavior of the filter nearby the edge center. The first two criteria can be trivially maximized as follows. From the Schwarz inequality for integrals, he showed that SNR (3) is bounded above by

$$n_0^{-1} \int_{-w}^{+w} G^2(x) dx \tag{12}$$

and localization of $E[x_0^2]$ by $n_0^{-1} \int_{-w}^{+w} G'^2(x) dx$ (13)

Both bounds are attained, and the product of SNR and localization of $E[x_0^2]$ is maximized when $f(x) = G(-x)$ in $[-W, W]$.

These maxima are so close together that it is not possible to select one as the response to the step while identifying the others as noise. There is need to add to our criteria the requirement that the function f so that it will not have "too many" responses to a single step edge in the vicinity of the step. There is need to limit the number of peaks in the response so that there will be a low probability of declaring more than one edge. Ideally, Canny would like to make the distance between peaks in the noise response approximate the width of the response of the operator to a single step. This width will be some fraction of the operator width W .

In order to express this as a functional constraint on f , there is the need to obtain an expression for the distance between adjacent noise peaks. First, noting that the mean distance between adjacent maxima in the output is twice the distance



between adjacent zero-crossings in the derivative of the operator output. Then making use of a result that the average distance between zero-crossings of the response of a function g to Gaussian noise is;

$$x_{ave} = \pi \left(\frac{-R(0)}{R''(0)} \right)^{1/2} \quad (14)$$

Where $R(\tau)$ is the autocorrelation function of g . In the case of looking for the mean-zero crossing spacing for the function f' , since

$$R(0) = \int_{-\infty}^{+\infty} g^2(x) dx \text{ and } R''(0) = - \int_{-\infty}^{+\infty} g''^2(x) dx \quad (15)$$

the mean distance between zero-crossings of f' will be;

$$x_{zc}(f) = \pi \left(\frac{\int_{-\infty}^{+\infty} f'^2(x) dx}{\int_{-\infty}^{+\infty} f''^2(x) dx} \right)^{\frac{1}{2}} \quad (16)$$

The distance between adjacent maxima in the noise response of f , denoted x_{max} , will be twice x_{zc} . Setting this distance to be some fraction k of the operator width.

$$x_{max}(f) = 2x_{zc}(f) = kW \quad (17)$$

This is a natural form for the constraint because the response of the filter will be concentrated in a region of width $2W$, and the expected number of noise maxima in this region is N_n where;

$$N_n = \frac{2W}{x_{max}} = \frac{2}{k} \quad (18)$$

Fixing k fixes the number of noise maxima that could lead to a false response.

3.5 Segmentation (Iris Detection)

It is at this stage that the iris boundary and the pupil boundary are marked or highlighted by a circle. In detecting circles, circular Hough transform was used. The Hough Transform can be described as a transformation of a point in a 2 dimensional region to a parameter space, dependent on the shape of the objects to be identified. The basic functionality of the Hough Transform is to detect straight lines. A straight line in the x, y -plane is described by (Fatoumata, 2010):

$$y = m * x + b \quad (19)$$

This line is represented in the Cartesian coordinate system by its parameters b and m (where m is the slope and b is the intercept). Due to the fact that perpendicular lines to the x -axis can give unbounded values for parameters m and b (b and m rises to infinity), lines are parameterized in terms of theta θ and r such that:

$$r = x * \cos(\theta) + y * \sin(\theta), \text{ for } \theta \in [0, \pi] \quad (20)$$

Where r is the distance between the line and the origin, θ is the angle. Thus, given x and y , every line passing through point (x, y) can uniquely be represented by (θ, r) . Both θ and r have finite sizes. The distance r will have the maximum value of two times the diagonal of the image. An edge detector is commonly used to provide a set of points that represents the boundaries in the image space. Unlike the linear HT (Hough Transform), the CHT (Circular Hough Transform) relies on equations for circles (Ioannou et.al., 1999). The equation of the a circle is,

$$r^2 = (x-a)^2 + (y-b)^2 \quad (21)$$

Here a and b represent the coordinates for the center, and r is the radius of the circle. The parametric representation of this circle is

$$x = a + r * \cos(\theta) \quad (22)$$

$$y = b + r * \sin(\theta) \quad (23)$$

In contrast to a linear Hough Transform, a Circular Hough Transform relies on 3 parameters (Nitasha et.ai 2012), which requires a larger computation time and memory for storage, increasing the complexity of extracting information from our image.

3.6 Cropping

After the segmentation, we then know the region of interest. Then the idea of getting rid of regions not needed comes to mind. To remove this region the iris image was cropped using an algorithm stated below:

- a) Scan the pixels from left to right, starting from the top.
- b) Record the first pixel that is not black and end the loop in (a).
- c) Repeat (a) from left to right, starting from the bottom.



- d) Repeat step (b) and end loop (c).
- e) Repeat (a) from top to bottom, starting from the left.
- f) Repeat (b) and end the loop at (e).
- g) Repeat (e) from top to bottom, starting from the right.
- h) Repeat (b) and end loop (g).
- i) Copy the pixel in the range gotten from (b), (d), (f) and (h) above into a new matrix.

3.7 Normalization

The remapping of the iris image $I(x; y)$ from raw Cartesian coordinates $(x; y)$ to the dimensionless nonconcentric polar coordinate system $(r; \theta)$ can be represented as (Sunita, 2012):

$$I(x(r, \theta), y(r, \theta)) \rightarrow I(r, \theta) \quad (24)$$

$$\text{with } x(r, \theta) = (1 - r)x_p(\theta) + rx_i(\theta) \quad (25)$$

$$y(r, \theta) = (1 - r)y_p(\theta) + ry_i(\theta) \quad (26)$$

$I(x, y) = \text{irisimage}$

$(x, y) = \text{originalcartesiancoordinates}$

$(r, \theta) = \text{normalisedcoordinates}$

$(x_p, y_p) = \text{pupilcoordinates}$

$(x_i, y_i) = \text{iriscoordinatesalong}\theta\text{direction.}$

3.8 Features Extraction

Features extraction is necessary to form the uniquely ordered sequence of features called iris signature from the iris image. If it is assumed that everything is known about the function (i.e. there is a formula for it), then such a sequence, of whatever length is desired, can easily be obtained by considering a function called the father wavelet. The Haar father wavelet is defined in (Maidstone, 2012).

Definition: The Haar father wavelet is defined as follows:

$$\phi(x) = \begin{cases} 1 & x \in [0,1] \\ 0 & \text{o/w} \end{cases} \quad (27)$$

Then the father wavelet coefficients can be computed as follows:

Definition: For a required level 2^j the father wavelet coefficients $c_{j,k}$ for $k \in \{1, \dots, j\}$ can be obtained by:

$$c_{j,k} = \int f(x) 2^{\frac{j}{2}} \phi(2^j x - k) dx \quad (28)$$

In general a wavelet transform is defined by two functions. The father wavelet which provides information about the scale of the wavelet and the mother wavelet which characterizes the shape.

3.9 Matching (Comparism)

The comparism of the extracted features (feature vectors) is needed in order to know whether they are similar (the right person) or not. The chi-squared model was used for the comparism (matching) of the features vectors.

$$D(I, J) = \frac{(\text{observedfeature} - \text{expectedfeature})^2}{(\text{expectedfeature})} \quad (29)$$

which can also be written as

$$D(I, J) = \sum_{i=1}^n \frac{(f(i; I) - f^\Delta(i))^2}{f^\Delta(i)} \quad (30)$$

In the equation above, I and J are the two features and $f(i; I)$ specifies the observed feature (current) where $f^\Delta(i)$ represents the expected feature. n is the number of the bins. The expected feature is expressed as;

$$f^\Delta(i) = \frac{f(i; I) + f(i; J)}{2} \quad (31)$$

In the equation above, $f(i; J)$ represents the previous feature extracted. The chi-squared value determines the level of correlation or similarity between the two iris images. A perfect match is zero and a total mismatch is unbounded.

3.10 Template Design

A template is a text file that can be viewed by any conventional text editor. The template of an individual iris contains information extracted from the iris image (i.e. the iris signature). The templates are saved in the iris folder created in the My Document folder. Information saved in the template includes; Name, Sex, Age and Extracted feature.

4.0 SYSTEM IMPLEMENTATION

Matlab is a simple and useful high-level language for matrix manipulation. Since images are matrices of numbers, many vision algorithms are naturally implemented in Matlab. It is often convenient to use Matlab for programs which other language is not ideal for in terms of data structures and constructs.

Edge detection: The image depicted in Figure 1 shows the output of the Canny edge detector (James, (2005) which takes in as input a gray image (or an RGB image) and produces a binary image as output.



Figure 1: The Edge Image

Segmentation: The image depicted in Figure 2 displays the output of the segmentation phase with the blue line showing the detected iris boundary and the red line showing the detected pupil boundary.

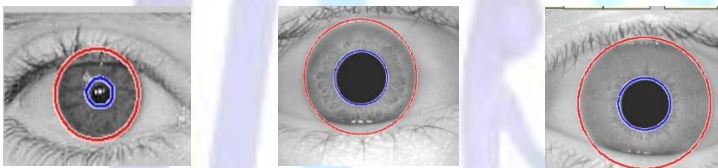


Figure 2: The Boundary Detected

Cropping: After which the image was cropped isolating (see Figure 3) only the needed region and turning the other region to black (i.e. zero pixels).

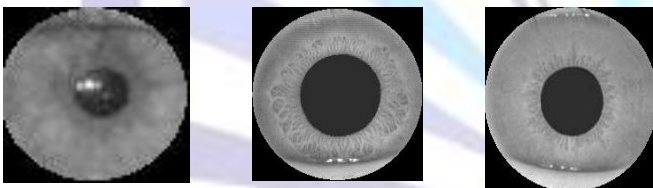


Figure 3: The Cropping of the Image

Normalization: The image depicted in Figure 4 shows the output of one of the normalized images to the dimension of 32 x 280 (in pixel).



Figure 4: The Normalized Iris Image

Features extraction: For the extraction of the features from the Normalized iris image, 2D wavelet transform (Sifuzzaman et.al., 2009) was used. Wavelet transform is a mathematical tool used to explore functions, analyze data and analyze image. 2D wavelet transform involves the use of high pass and low pass filters to characterize the father and mother wavelet (Robert, 2012).

At the end of this stage, the Horizontal coefficient (cH), vertical coefficient (cV), diagonal coefficient (cD), and the Absolute coefficients (cA) was obtained. A reduced version of data obtained is stated below.

**Table 1: cA (absolute coefficient)**

ABSOLUTE COEFFICIENT															
282	278	270.5	274.5	265.5	267.5	271	277	283	273	277.5	269.5	273	286	286	283.5
302.5	284.5	275	270	265.5	271	276	276	280.5	279.5	278.5	277.5	283.5	287.5	287	276
317.5	294	285.5	278.5	280.5	281.5	283.5	274	276.5	294	287.5	284.5	292	292.5	288	272
304.5	293	290.5	282.5	289	280.5	287.5	283	284	302.5	295.5	291	289	280.5	277	272
291	289	284	286	288.5	278.5	276.5	274.5	280	293.5	291.5	288.5	272	267	261	267.5
290	285.5	275.5	276.5	275.5	268.5	272.5	276	281	285	282	275.5	262.5	273	270	269.5
291.5	285	276.5	272	276.5	270	277	286	286.5	281	285.5	273	256.5	267	273.5	274
295	290	282.5	266.5	277.5	271	281.5	292.5	286	278.5	291.5	272.5	258	263	269	275.5
293	291	284.5	262	277	271	281	287.5	277.5	272.5	289.5	266	259.5	257.5	262	270.5
283.5	280.5	286	269.5	270	268	279.5	279.5	273	270	280.5	257	254	253	258	268.5
277	275	286.5	273	267	263.5	275.5	278	272.5	268.5	268	253.5	253	253.5	262.5	268.5
272	271.5	285.5	273	265	259	266	269.5	271.5	271	268.5	263.5	259	254	260	257
270	268	281	269	265	257	258	263	271	273.5	274	274	269	255	255	247
269	265	275	265	265	259	260.5	265	270.5	267.5	268	269.5	273	260.5	261.5	254
274.5	273	279	274	270	259	256.5	260	266	260.5	260	274	274	262	260	254
273	271	278	276.5	268	259	256.5	260	264.5	260	257	265.5	264.5	258.5	258.5	251

5. RESULT

The performance of the iris system is stated below in terms of computational speed, robustness and performance. The overall computational time taken by the system for enrollment is less than a minute (42seconds). The Daugman's system was tested under several environments recording 99.94% accuracy with FAR (false acceptance ratio) of 0.00% and an FRR (false rejection ratio) of 0.13%. Liet.al, (2003) recorded an FAR of 0.00% with an FRR of 0.87% while Tan et al (2003) recorded an FAR of 0.00%, an FRR of 1.03% (Vatsa, 2005). In Table 1, 300 true irises were tested on the system, 2 were rejected. 270 false irises were tested against the system and none was accepted. The designed system has a FAR (False accepting ratio) of 0.00 and an FRR (False rejection ratio) of 0.6667.

However, the presence of eyelid occlusion or eyelashes in the iris region can cause an (despite the reduction in radius of the iris boundary) incorrect boundary detection. Incorrect boundary detection of normalized image significantly increases the probability of false rejection. Further complications, which had an impact on the system's performance was caused by the shape of iris or pupil - elliptical instead of circular.

Implementing the design on the Uiris V1 requires changing some of our parameter such as the radius to search for pupil (9 15) and iris boundary (28 60) and the Sigma (0.8) in order to get the desired outcome. Applying (ICA) Independent Component Analysis algorithm to the same iris image tested above, a FRR of 1.6667% and FAR of 0% was obtained.

6. CONCLUSION

In conclusion, there is a limit to which mathematical models can enhance image quality and hence the performance of the system is still dependent on the quality of the hardware used for the acquisition of the iris image. The level of accuracy of iris recognition has a lot to do with the segmentation of the iris region. Removal of eyelids and eyelashes enhances the accuracy to the system. The proposed system achieved a high accuracy. For the future work the image segmentation techniques or noise removal methods can be improved, so that the input image to the feature extraction stage could be made better which can improve the final outcome. Also, the reduction in the computational complexity of the models used is important.

References

1. Bakstein Eduard (2013). "Iris Recognition", Retrieved from https://cw.fel.cvut.cz/wiki/media/courses/a6m33bio/iris_1-4-2014.pdf. Accessed in August, 2014.
2. Boles W. and Boashash B. (1998). "A human identification technique using images of the iris and wavelet transform", IEEE Trans. Signal Process. 46(4):1185-1188.
3. Canny John (1986). "A Computational Approach to Edge Detection", IEEE Transactions on Pattern Analysis and Machine Intelligence. 8(6).



4. Choi Seung-Seok, Yoon Sungsoo, Cha Sung-Hyuk and Tappert Charles C. (2010). "Use of histogram distances in Iris Authentication", ICGST-GVIP Journal, 5(5).
5. Daugman J. (1993). "High confidence visual recognition of persons by a test of statistical independence", IEEE Trans. PAMI, 15: 1148-1161.
6. Daugman J. (2004), How Iris Recognition Works, IEEE Transactions on Circuits and Systems for Video Technology, 14(1): 21-30. John Daugman's webpage, Cambridge University, Faculty of Computer Science & Technology, Cambridge. <http://www.cl.cam.ac.uk/~jgd1000/>. Accessed 12 May 2015
7. Daugman J. (2007). "New methods in iris recognition", IEEE Transactions on Systems, Man, and Cybernetics – Part B: Cybernetics. 37(5):1167–1175.
8. Poonam Dhankhar and Neha Sahu (2013). "A Review and Research of Edge Detection Techniques for Image Segmentation", International Journal of Computer Science and Mobile Computing (IJCSMC).2(7);86 – 92.
9. Pierre Gravel, Gilles Beaudoin, and Jacques A. Guise. De (2004). "A Method for Modeling Noise in Medical Images", IEEE Transactions On Medical Imaging, 23(10).
10. Gulmire Kshamaraj, Ganorkar Sanjay (2012). "Iris Recognition Using Independent Component Analysis", International Journal of Emerging Technology and Advanced Engineering Website: www.ijetae.com ISSN 2250-2459.2(7).
11. He Zhaofeng, Tan Tieniu, Sun Zhenan and Qiu Xianchao, (2008). "Towards Accurate and Fast Iris Segmentation for Iris Biometrics", Pattern Analysis and Machine Intelligence (Transactions on IEEE), 31(9).
12. Ioannou Dimitrios, Huda Walter, Laine Andrew F. (1999). "Circle recognition through a 2D Hough Transform and radius histogramming", Image and Vision Computing, 17: 15–26.
13. Jain A. K., Hong L., Pankanti S., and Bolle R. (1997). "An Identity-Authentication System Using Finger-prints", In Proceeding of the IEEE. 85: 1365-1388.
14. James, Matthew (2005). "An Introduction to Edge Detection". Retrieved from www.generation5.org/content/2002/im01.asp. Accessed on Aug 2014.
15. Jin Qiuchun, Tong Xiaoli, Ma Pengge and Bo Shukui (2013). "Iris Recognition by New Local Invariant Feature Descriptor", Journal of Computational Information Systems. 9(5).
16. Kaur Gaganpreet, Girdhar Akshay, Kaur Manvjeet (2010). "Enhanced Iris Recognition System", International Journal of Computer Applications (0975 – 8887).8(1).
17. Kekre.H.B.,Thepade Sudeep D., Jain Juhi and Agrawal Naman (2010). "Iris Recognition using Texture Features Extracted from Haarlet Pyramid", International Journal of Computer Applications (0975 – 8887), 11(12).
18. Khan Mohd Basheer, Lavanya P. (2013). "Advanced Secured Vehicle System with Iris Technology and Auto Speed", Advanced Secured Vehicle System with Iris Technology and Auto Speed. ISSN: 2321-9939.
19. Konduri Harsha and Samrat Sai (2012). "Canny Edge Detection", Retrieved from www-student.cse.buffalo.edu/~sreehars/images/CANNY_REPORT.pdf. Accessed on May 24, 2015.
20. Li Ma, Tieniu Tan, Yunhong Wang and Dexin Zhang (2003). "Personal Identification Based on Iris Texture Analysis", IEEE Transactions on Pattern Analysis and Machine Intelligence, 25(12): 1519- 1533.
21. Maidstone Robert (2012). "Wavelets in a Two-Dimensional Context", Retrieved from www.lancaster.ac.uk/pg/maidston/FinalReport.pdf on Aug 2014. Algorithm for grey image retrieved from <http://www.mathworks.com/help/matlab/ref/rgb2grey.html>, accessed 26 May 2015.
22. Monaheng Matsoso Samuel and Kuruba Padmaja (2013). "Iris Recognition Using Circular Hough Transform", International Journal of Innovative Research in Science, Engineering and Technology;2(8).
23. Mythili C., Karitha V. (2011). "Efficient Technique for Colour Image Noise Reduction", The Research Bulletin of Jordan ACM, 2(3): 41-44.
24. Nitasha, Sharma Shammi and Sharma Reecha (2012). "Comparison between Circular Hough Transform And Modified Canny Edge Detection Algorithm For Circle Detection", International Journal of Engineering Research & Technology (IJERT); 1(3).
25. Patil C.M., Patilkulkarani and Sudarshan (2009). "An Approach of Iris Feature Extraction for Personal identification", In Proceedings of ISCO at Coimbatore, pg. 43.
26. Rydgren Erik, Ea Thomas, Amiel Frédéric, Rossant Florence and Amara Amara(2004). "Iris Features Extraction Using Wavelet Packets", Institut Supérieur d' Electronique de Paris, ISEP 21 rue d'Assas 75270 Paris Cedex 06.
27. Sifuzzaman M., Islam M. R., and Ali M. Z. (2009). "Application of Wavelet Transform and its Advantages Compared to Fourier Transform", Journal of Physical Sciences. 13:121-134.



28. Tan T., Ma L., Wang Y. and Zhang D. (2003). "Personal Identification based on Iris Texture Analysis", IEEE Transactions on Pattern Analysis and Machine Intelligence, 25(12): 1519-1533.
29. Vatsa M., Singh R., and Noore A. (2005). "Reducing the False Rejection Rate of Iris Recognition Using Textural and Topological Features", International Journal of Signal Processing 2. (ISSN: 1304-4494).
30. Wildes R. (1997). "Iris recognition: an emerging biometric technology". Proceedings of the IEEE, 85(9):1348-1363.
31. Wildes R., Asmuth J., Green G., Hsu S., Kolczynski R., Matey J. and McBride S. (2011). "A system for automated iris recognition", Proceedings IEEE Workshop on Applications of Computer Vision, Sarasota, FL. Pp. 121-128.

